ACS SyntheticBiology

pubs.acs.org/synthbio

Technical Note

Evaluating Capture Sequence Performance for Single-Cell CRISPR Activation Experiments

Xin Yi Choo, Yu Ming Lim, Khairunnisa Katwadi, Lynn Yap, Karl Tryggvason, Alfred Xuyang Sun, Shang Li, Lusy Handoko, John F. Ouyang,* and Owen J. L. Rackham*

Cite This: *ACS Synth. Biol.* 2021, 10, 640–645

Read Online

ACCESS | Metrics & More | Article Recommendations | Supporting Information

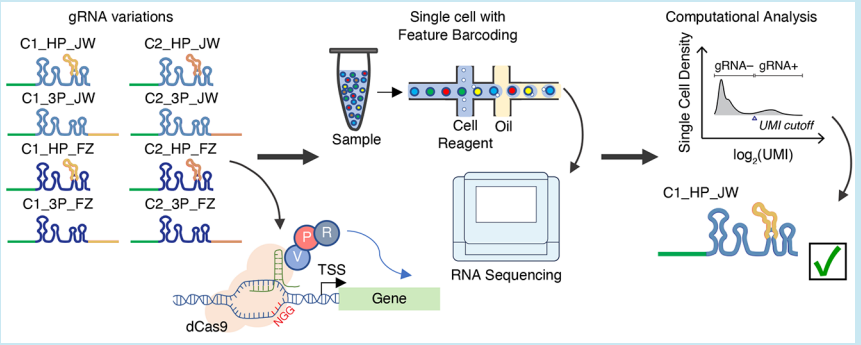

ABSTRACT: The combination of single-cell RNA sequencing with CRISPR inhibition/activation provides a high-throughput approach to simultaneously study the effects of hundreds if not thousands of gene perturbations in a single experiment. One recent development in CRISPR-based single-cell techniques introduces a feature barcoding technology that allows for the simultaneous capture of mRNA and guide RNA (gRNA) from the same cell. This is achieved by introducing a capture sequence, whose complement can be incorporated into each gRNA and that can be used to amplify these features prior to sequencing. However, because the technology is in its infancy, there is little information available on how such experimental parameters can be optimized. To overcome this, we varied the capture sequence, capture sequence position, and gRNA backbone to identify an optimal gRNA scaffold for CRISPR activation gene perturbation studies. We provide a report on our screening approach along with our observations and recommendations for future use.

KEYWORDS: *CRISPR activation, hESC, overexpression, transcription factors, single-cell RNA-seq, feature barcoding technology*

INTRODUCTION

The widespread uptake of single-cell RNA sequencing (scRNA-seq) has resulted in a shift in the way that we study biology. Now, it is possible not only to characterize gene expression at the single-cell resolution (e.g., the Human Cell Atlas[1]) but also to study genetic and gene-expression perturbations at the single-cell level (e.g., refs 2 and 3). To achieve this, homologous recombination-based methods have been widely adopted for gene targeting,[4] and of these, CRISPR/Cas9, an RNA-guided endonuclease enzyme, has been extensively utilized. This is largely due to its compatibility with multiple species, relative simplicity to use, and flexibility. In particular, the CRISPR activation (CRISPRa) system for activating gene expression[5] utilizes guide RNAs (gRNAs) to target a dead Cas9(dCas9) protein fused to a transactivation domain (e.g., VPR,[6] SAM,[7] or SunTag[8]) to induce endogenous gene expression at specific genomic loci. Recently, several advances have been made in the design of gRNAs. They include the construction of the genome-wide CRISPRa and CRISPR inhibition (CRISPRi) gRNA libraries targeting all known coding genes,[9,10] the alteration of the protospacer sequence to tune the degree of gene activation or inhibition,[11] and the inclusion of unique molecular identifiers (UMIs) in gRNA to perform lineage tracing of pooled CRISPR screens.[12] gRNAs were also modified for use with single-cell technologies through the addition of guide barcode expression cassettes (e.g., Perturb-seq[3] and CRISP-seq[13]) and modification of the gRNA scaffold to incorporate capture sequences that can be captured by complementary primers engineered into single-cell gel beads.[14,15]

As scRNA-seq solutions have become commercialized, they have become more readily accessible to the scientific

Received: October 1, 2020
Published: February 24, 2021

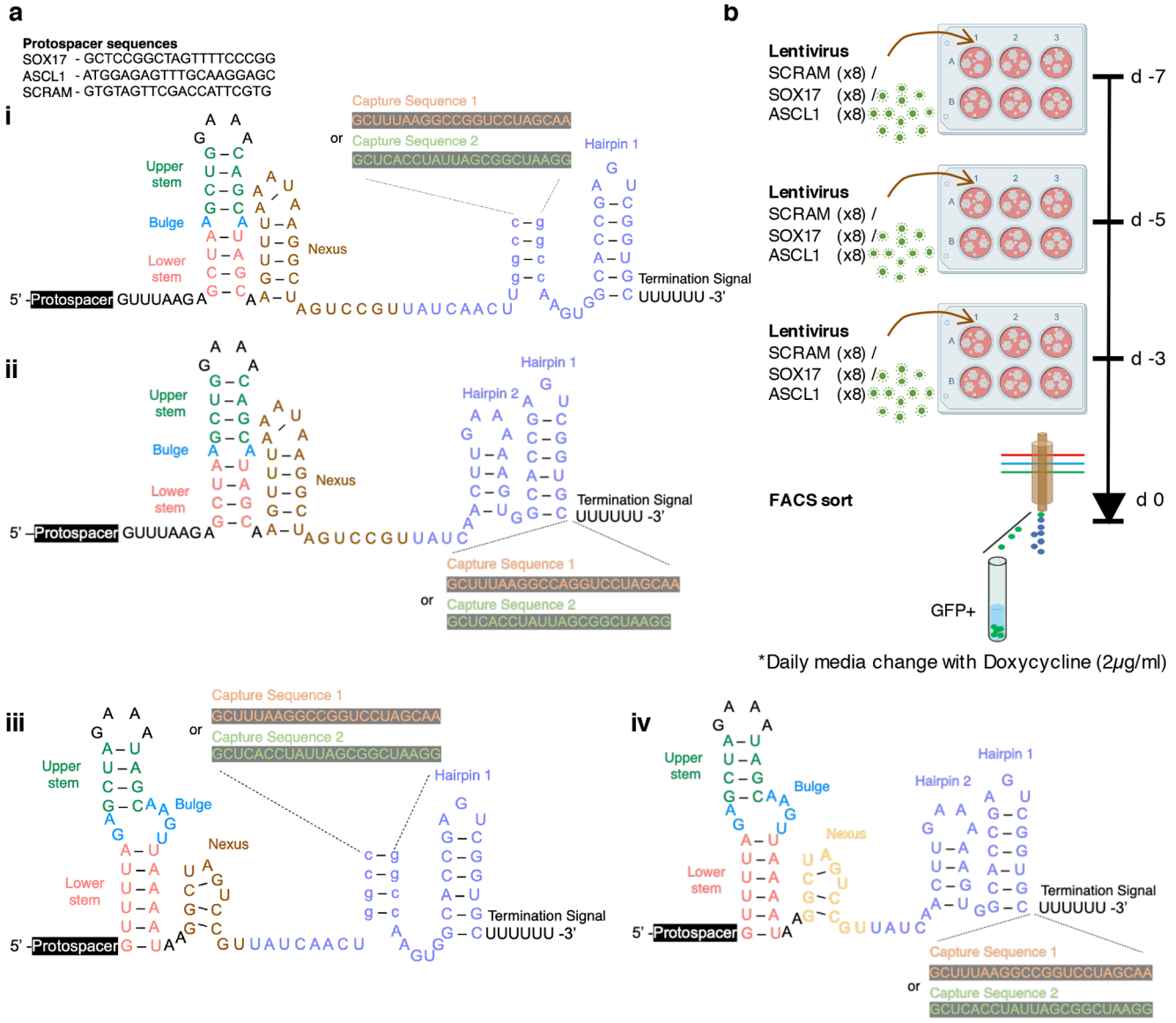

Figure 1. gRNA screening to identify the optimal gRNA scaffold for 10x chromium feature barcoding capture for single-cell RNA-seq application. (a) Schematics of unique gRNA scaffold designs: (i) depicting C1_HP_JW or C2_HP_JW, (ii) depicting C1_3P_JW or C2_3P_JW, (iii) depicting C1_HP_FZ or C2_HP_FZ, and (iv) depicting C1_3P_FZ or C2_3P_FZ. (b) Eight unique gRNA scaffolds containing the same protospacer sequence (SOX17, ASCL1, or SCRAM) were delivered together to induce dCas9-VPR *AAVS1* knock-in H1 cells (4K) by pooled *lentivirus*. Image created with BioRender.com. Cells were transduced in the presence of doxycycline for 3, 5, or 7 days prior to harvesting. Live/PI$^-$ and GFP$^+$ populations were sorted for scRNA-seq. Uninfected cells were also sorted for the live/PI$^-$ population as the scRNA-seq control.

community; subsequently, interest in identifying the best experimental design has grown. In particular, with the release of 10x Genomics' v3 chemistry with Feature Barcoding technology, it is now possible to capture both the polyadenylated mRNA (poly(A) mRNA) transcripts and other compatible targets of interest (e.g., gRNAs) from the same cell.[15] This is achieved by adapting the beads to include not only the poly(dT) primer (for mRNAs) but also two other primer sequences, known as capture sequences 1 and 2 (C1 and C2). The complement of these sequences can be incorporated into oligo-conjugated antibodies or gRNAs to recover their presence using sequencing. Before using this approach, a number of key experimental parameters need to be set for the gRNA scaffold design. In addition to choosing between C1 and C2, the location of the capture sequence can be in one of two places within the gRNA sequence, namely, at a hairpin (HP) location or at the three-prime (3P) end. Furthermore, the delivery of these gRNAs is routinely done by using a lentiviral system, the structure of which varies (e.g., refs 3 and 16), and this can also affect experimental outcomes. We have systematically tested each combination for the over-expression of two genes (ASCL1 and SOX17) and drawn conclusions about the effect of each choice on (1) the capture efficiency of the gRNA, (2) the efficiency of the CRISPRa, and (3) the transduction efficiency.

One of the key advances that this technology prevails is in facilitating pooled screens where many different perturbations are carried out in a single population of cells prior to deconvolution by scRNA-seq, returning both the gene expression profile and perturbations present in each cell individually. As a result, we have carried out this study using

https://dx.doi.org/10.1021/acssynbio.0c00499
ACS Synth. Biol. 2021, 10, 640−645

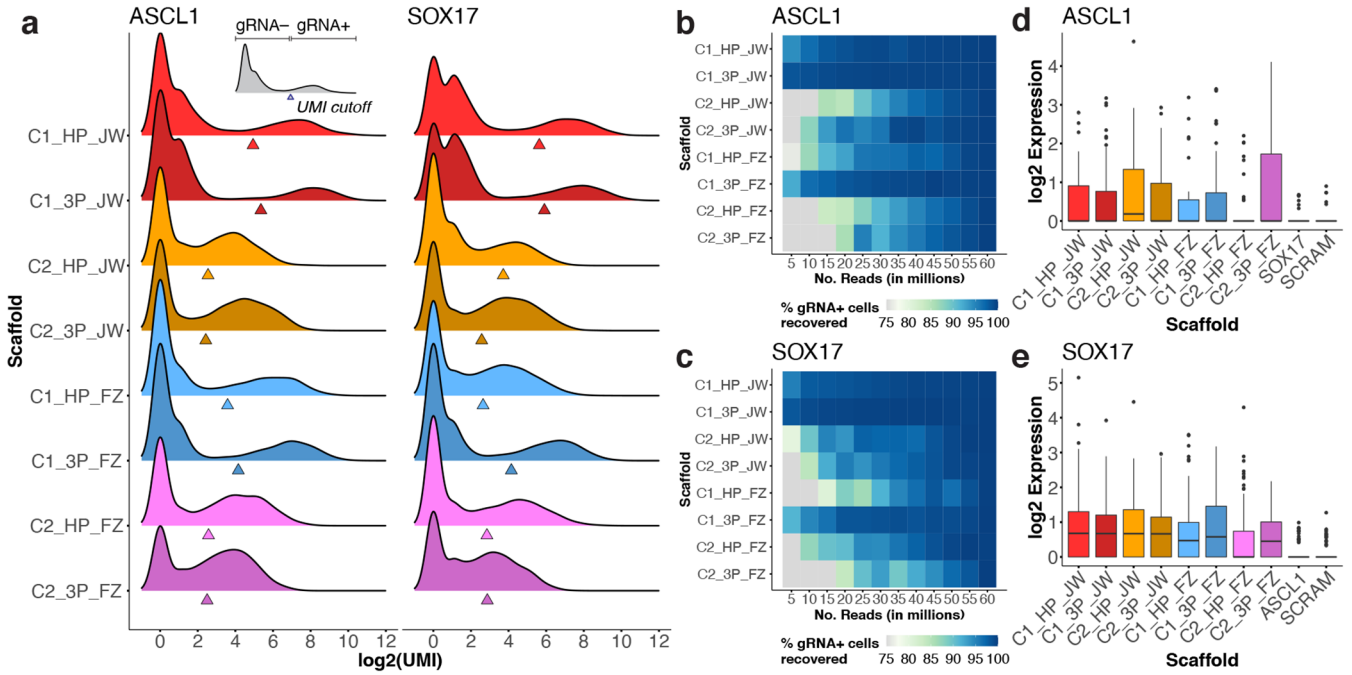

Figure 2. Identification of the optimal gRNA scaffold for single-cell transcription factor (TF) overexpression by quantifying the capture efficiency by the 10x Genomics single-cell assay and overexpression efficiency. (a) Distribution of log2(UMI) for each scaffold across single cells for both ASCL1 and SOX17. A Poisson−Gaussian mixture model is fitted to each distribution to determine a cutoff (triangles) separating gRNA− and gRNA+ cells (see the inset for an illustration), with a higher cutoff being better. (b,c) Proportion of gRNA+ cells recovered for (b) ASCL1 and (c) SOX17 upon downsampling the gRNA library in terms of the sequencing depth, that is, the number of reads. (d) Single-cell gene expression of ASCL1, in log2(normalized UMIs), across different ASCL1 gRNA scaffolds, SOX17 gRNA+ cells, and SCRAM gRNA+ cells. (e) Single-cell gene expression of SOX17, in log2(normalized UMIs), across different SOX17 gRNA scaffolds, ASCL1 gRNA+ cells, and SCRAM gRNA+ cells.

similar conditions to ensure that the results are applicable to all uses of this technology.

RESULTS

To systematically test the effect of different gRNA scaffold design choices, we varied a number of parameters as follows (Figure 1a, Supplementary Table S1):

1) We chose two different gRNA protospacer sequences that had previously been shown to increase the expression of *ASCL1*[17] and *SOX17*[18] as well as a scrambled control (denoted as SCRAM from hereafter).
2) We varied the capture sequence between C1 and C2.
3) We varied the position of the capture sequence between an HP and a terminal 3P location
4) We varied the delivery construct between two commonly used gRNA backbones by the Jonathan Weissman (JW) group[3] and the Feng Zhang (FZ) group.[16]

This resulted in a total of 24 different experimental setups (three protospacers and eight scaffolds), each identified based on these combinations, for example, ASCL1-C1_HP_JW.

To begin, we engineered and validated a human embryonic stem cell (hESC) to express the dCas9-VPR in a doxycycline-inducible manner (referred to as 4K, Supplementary Figure 1a,b), as described in ref 19. Next, for each of the protospacers, we introduced each possible combination of capture sequence, position, and delivery construct. To allow the overexpression of SOX17 and ASCL1 to occur, we cultured these cells in the presence of doxycycline before collecting them at three time points (D3, D5, and D7), and an unstimulated control was also collected (Figure 1b). By day 3, we had already observed ∼29.7% guide-positive cells, and this proportion remained constant throughout (Supplementary Figure S2a,b). As such, we combine the data from across the time series for the purposes of comparing the gRNA scaffolds. These cells were subjected to scRNA-seq, resulting in a data set of 13 743 cells, robustly detecting 13 042 genes (Supplementary Figure S3a). The data from each cell were processed to generate a gene expression profile as well as to identify which of the 24 protospacer−scaffold combinations were present (Supplementary Figure S3b and Supplementary Methods). These results were then analyzed to identify which gRNA combination was the most effective.

Ability to Detect gRNAs. For each gRNA scaffold across the different protospacers, we compared the ability to distinguish between cells that were likely gRNA-positive from those from which the detection might be a result of noise (possibly due to the capture of ambient gRNA). We did this by fitting a Poisson−Gaussian mixture model to the number of UMIs (or specifically $\log_2$(UMI)) detected for each combination (Supplementary Figure S3c). We then calculated the UMI cutoff at which it was possible to distinguish the Gaussian-distributed counts (the signal, gRNA+ cells) from the Poisson counterpart (the noise, gRNA− cells). We found that the C1_3P_JW and C1_HP_JW scaffolds had the best performance, with the highest UMI cutoffs (Figure 2a, Supplementary Figure S3d). Furthermore, the cells containing the C1_3P_JW and C1_HP_JW scaffolds had a substantially higher distribution of gRNA UMIs (Supplementary Figure S3e). Overall, the majority of the single cells contained only a single protospacer with a similar number of cells distributed across the three different protospacers (Supplementary Figure S3f,g). We further quantified the ability to detect the gRNAs

https://dx.doi.org/10.1021/acssynbio.0c00499
ACS Synth. Biol. 2021, 10, 640−645

Table 1. Ranking of the Different Scaffolds Tested in This Study[a]

	ability to detect gRNA			ability to induce overexpression			
scaffold	UMI cutoff	% cells recovered	rank	log2FC	% cells expressed	rank	overall rank
C1_HP_JW	good	good	2	good	good	2	1
C1_3P_JW	good	good	1	good	OK	4 (tied)	2
C2_HP_JW	OK	OK	4 (tied)	v. good	good	1	3
C2_3P_JW	poor	OK	6	OK	good	4 (tied)	5
C1_HP_FZ	OK	OK	4 (tied)	OK	poor	7	7
C1_3P_FZ	good	good	3	good	OK	4 (tied)	4
C2_HP_FZ	poor	OK	7	poor	poor	8	8
C2_3P_FZ	poor	poor	8	good	OK	3	6

[a]First, the scaffolds are evaluated based on the detection efficiency by the 10x system in terms of the UMI cutoff for gRNA+ cells and the proportion of cells recovered upon downsampling the reads in the gRNA library. Second, the scaffolds are assessed based on their ability to overexpress the target gene in terms of the log2 fold change (log2FC) in the expression and proportion of cells expressing the target gene. Each of the four evaluation criteria was ranked (Supplementary Table S2), and these ranks were averaged across the two categories (gRNA detection and overexpression efficiency) to generate the corresponding ranks. All four ranks were also combined to give the overall rank to determine the optimal scaffold for single-cell transcription factor overexpression. See Supplementary Table S2 for a more detailed breakdown.

by downsampling the number of reads in the gRNA library and recovering the gRNA+ cells using the same Poisson−Gaussian mixture approach. Again, the C1_3P_JW and C1_HP_JW scaffolds were the most robust toward downsampling, retaining >90% of the gRNA+ cells even at less than a tenth of the original sequencing depth of roughly 60 million reads (Figure 2b,c). Overall, the C1_3P_JW and C1_HP_JW scaffolds had the best performance in the ability to detect gRNAs.

Ability to Induce Robust Changes in Expression. Next, we compared the ability of each of the gRNA scaffolds containing the ASCL1 and SOX17 protospacers to induce a change in the expression of the gRNA targets as compared with the SCRAM control (Figure 2d,e). Overall, we observed a robust overexpression of ASCL1 and SOX17 with the exception of the C2_HP_FZ scaffold. The C2_HP_JW scaffold had the largest fold increase in expression (average log2 fold change of 1.31), whereas the C1_HP_JW, C1_3P_JW, C1_3P_FZ, and C2_3P_FZ scaffolds performed well (average log2 fold change of 0.96 to 1.08). Apart from the average change in expression, we also examined the proportion of single cells expressing the target gene. The C1_HP_JW, C2_HP_JW, and C2_3P_JW scaffolds had the highest proportion of cells expressing ASCL1 or SOX17 (average proportion of 58.1 to 58.8%, Supplementary Table S2). On the whole, the C2_HP_JW and C1_3P_JW scaffolds had the best performance in the ability to induce robust changes in expression.

Efficiency of Transduction. We then investigated whether the choice of gRNA scaffold affects how well the gRNA gets transduced into the hESC. For single cells containing only a single type of scaffold, we observed a similar number of cells across the different scaffolds tested (Supplementary Figure S3i), suggesting that the transduction efficiencies were comparable. This is in agreement with Supplementary Figure S2b, where the proportions of GFP/gRNA+ cells after transduction are similar across scaffolds. We do note that the number of cells observed for each scaffold was dependent on (i) the capture efficiency by the 10x system, (ii) the number of cells loaded into the 10x system, and (iii) the multiplicity of infection (MOI). Thus it is difficult to rank the scaffolds in terms of transduction efficiency. Nonetheless, the similar number of GFP/gRNA+ cells observed and the robust overexpression were indicative of the successful transduction of the gRNA.

Identification of Optimal gRNA Scaffold. To determine the optimal gRNA scaffold, we evaluated the performance of the gRNA based on (i) the ability to detect the gRNA by the single-cell assay and (ii) the ability of the gRNA to induce overexpression (Table 1). For the gRNA detection, we compared the UMI cutoff for gRNA+ cells (Figure 2a, Supplementary Figure S3d) and the proportion of gRNA+ cells recovered from downsampling reads (Figure 2b,c). For overexpression efficiency, we examined the log2 fold change (log2FC) in the expression of the target gene and the proportion of cells expressing the target (Figure 2d,e). Each of these four evaluation criteria was ranked, and these ranks were averaged to identify the optimal gRNA scaffold. We found that the overall best performance was achieved when using C1 positioned in the HP of the gRNA and using the construct from Jonathan Weissman group (C1_HP_JW scaffold).

Furthermore, to demonstrate that the C1_HP_JW scaffold is effective in different cell lineages, we performed trilineage differentiation (Supplementary Figure S4a) of 4K hESCs to ectodermal (OTX2$^+$, Supplementary Figure S4d), endodermal (SOX17$^+$, Supplementary Figure S4e), and mesodermal (BRACHYURY$^+$, Supplementary Figure S4f) progenitor cells for transduction with ASCL1-C1_HP_JW *lentivirus*. By real-time polymerase chain reaction (RT-PCR), we observed that ASCL1 mRNA overexpression was achieved in all three cell lineages (Supplementary Figure S4g−i). This indicates that the application of the optimized gRNA scaffold can be extended beyond pluripotent cells.

DISCUSSION

As the technologies for both sequencing RNA and perturbing gene expression in single cells become more sophisticated, our ability to explore more complex biological questions also follows. However, these experiments are often very time-consuming and very expensive to perform. It is therefore important to design experiments to maximize both data output quantity and quality. It is also worth noting that the target of the gRNA is an important feature and will affect the scale of gene activation. For CRISPRa systems, it is optimal for the protospacer to target a ∼100 nucleotide window upstream of the transcription start site (TSS).[20] Through the use of tools such as CRISPick[21] and CHOPCHOP,[22] these protospacer sequences can be easily identified and, as such, were not part of this survey.

https://dx.doi.org/10.1021/acssynbio.0c00499
ACS Synth. Biol. 2021, 10, 640−645

Here we tested the effect of the capture sequence, its position, and the scaffold used to deliver it to the cell. We then evaluated the performance of each gRNA combination based on (i) its ability to be detected by the 10x genomics single-cell assay and (ii) how well it could induce gene overexpression. This is one of the first studies of its kind, with previous comparisons being made using CRISPR or CRISPRi.[15] We found that the overall best performance is achieved when using C1 positioned in the HP of the gRNA and using the construct from the Jonathan Weissman group (C1_HP_JW scaffold, Table 1). A similar performance was seen by positioning the capture sequence at the 3P end of the gRNA (C1_3P_JW scaffold). We showed that the position of the capture sequence (HP/3P) does not affect the performance of the gRNA in terms of either the gRNA detection or the gene overexpression. This is in contrast with Replogle et al.,[15] where the incorporation of the capture sequence at the 3P end compromised the CRISPRi activity. Such differences could be due to inherent differences in the CRISPR mechanism (activation vs inhibition). We also found that C2 did not perform as well in either position, and in particular, the detection efficiency was much lower. These results are in agreement with what has been observed for C1 and C2 in a CRISPRi system.[15] Whereas our study is focused on gene activation using the VPR system, the findings are applicable for other CRISPRa systems such as SAM and SunTag. The gRNA detection efficiency is related to the gRNA interactions with the single-cell gel beads, which are independent of the choice of CRISPR machinery. The overexpression efficiency will depend on the binding between the DNA, gRNA, and dcas9 protein (where our observations hold) and the activator being used (i.e., VPR/SAM/SunTag). Thus the overexpression efficiency can vary depending on the choice of transcriptional activator. Notably, our observations corroborate those of a recent study[15] that tested several gRNA scaffolds in a CRISPRi experiment, suggesting that our findings are applicable to other types of CRISPR experiments.

Overall, these observations will be particularly important to consider when designing experiments. In particular, many currently available kits for use with the 10x genomics kit utilize C1, and thus it will be attractive to use the second capture sequence for the capture of gRNAs, but this could unduly affect the outcome of the experiment analysis. For example, if cell hashing[23] is performed using C1 to multiplex samples, then it leaves only C2 for the gRNA capture, and this could greatly reduce the capture efficiency of this critical experimental component.

■ ASSOCIATED CONTENT

Supporting Information

The Supporting Information is available free of charge at https://pubs.acs.org/doi/10.1021/acssynbio.0c00499.

Supplementary Methods: (1) hESC culture and stable cell line construction, (2) DNA isolation, PCR, and gel electrophoresis, (3) gRNA plasmid construction and *Lentivirus* generation, (4) gRNA *Lentivirus* transduction, (5) fluorescence-activated cell sorting (FACS), (6) single-cell RNA sequencing, (7) gRNA scaffold identification and analysis, (8) scRNA-seq gene expression analysis, (9) trilineage differentiation and ASCL1 gRNA *lentivirus* transduction, and (10) RNA extraction, cDNA synthesis, and RT-PCR. Supplementary Figures: (S1) Validation of the inducible dCas9-VPR *AAVS1* knock-in H1 clone (4K), (S2) FACS data, (S3) computational strategies for the identification of the optimal gRNA scaffold, results for the SCRAM gRNA, and additional results regarding the 10x capture efficiency, and (S4) testing gRNA efficiency in differentiated hESCs (PDF)

Supplementary Tables: (S1) Oligonucleotides for the generation of protospacer and gRNA scaffold variations used in this study, (S2) detailed values and ranks for different evaluation criteria for gRNA scaffolds, and (S3) PCR primers for validating dCas9-VPR and M2rtTA insertion at the AAVS1 locus (XLSX)

■ AUTHOR INFORMATION

Corresponding Authors

John F. Ouyang − *Program in Cardiovascular and Metabolic Disorders, Duke-NUS Medical School, Singapore 169857*; Email: john.ouyang@duke-nus.edu.sg

Owen J. L. Rackham − *Program in Cardiovascular and Metabolic Disorders, Duke-NUS Medical School, Singapore 169857*; orcid.org/0000-0002-4390-0872; Email: owen.rackham@duke-nus.edu.sg

Authors

Xin Yi Choo − *Program in Cardiovascular and Metabolic Disorders, Duke-NUS Medical School, Singapore 169857*; orcid.org/0000-0002-1783-0102

Yu Ming Lim − *Program in Cardiovascular and Metabolic Disorders, Duke-NUS Medical School, Singapore 169857*; orcid.org/0000-0001-8180-5705

Khairunnisa Katwadi − *Program in Cardiovascular and Metabolic Disorders, Duke-NUS Medical School, Singapore 169857*; orcid.org/0000-0002-7546-9546

Lynn Yap − *Program in Cardiovascular and Metabolic Disorders, Duke-NUS Medical School, Singapore 169857*; orcid.org/0000-0001-8206-9148

Karl Tryggvason − *Program in Cardiovascular and Metabolic Disorders, Duke-NUS Medical School, Singapore 169857*; orcid.org/0000-0002-0879-3290

Alfred Xuyang Sun − *National Neuroscience Institute, Singapore 308433; Genome Institute of Singapore, Singapore 138672*; orcid.org/0000-0002-7893-2006

Shang Li − *Program in Cancer and Stem Cell Biology, Duke-NUS Medical School, Singapore 169857*; orcid.org/0000-0002-6226-3362

Lusy Handoko − *Program in Cardiovascular and Metabolic Disorders, Duke-NUS Medical School, Singapore 169857*; orcid.org/0000-0001-7989-4243

Complete contact information is available at: https://pubs.acs.org/10.1021/acssynbio.0c00499

Author Contributions

O.J.L.R. conceptualized the study. O.J.L.R. and J.F.O. supervised the study. X.Y.C. planned, implemented, and analyzed the experimental aspects with support from Y.M.L., K.K., L.Y., K.T., A.X.S., S.L., and L.H. J.F.O. planned, implemented, and analyzed the computational aspects with assistance from O.J.L.R. O.J.L.R., J.F.O., and X.Y.C. wrote the manuscript with input from all authors. All authors approved of and contributed to the final version of the manuscript.

Notes

The authors declare no competing financial interest.

Single-cell sequencing data (including raw data and processed UMI counts matrix) have been deposited at the NCBI Gene Expression Omnibus (GEO) repository under accession number GSE164393.

■ ACKNOWLEDGMENTS

We acknowledge Novagene, the GIS single-cell sequencing service, and Sudhagar Samydurai for their help in the execution of this work. Some images were created with BioRender.com. X.Y.C., Y.M.L., K.K., J.F.O. and O.J.L.R. acknowledge support from the Singapore National Research Foundation Competitive Research Programme (NRF-CRP20-2017-0002).

■ REFERENCES

(1) Regev, A., Teichmann, S. A., Lander, E. S., Amit, I., Benoist, C., Birney, E., Bodenmiller, B., Campbell, P., Carninci, P., Clatworthy, M., Clevers, H., Deplancke, B., Dunham, I., Eberwine, J., Eils, R., Enard, W., Farmer, A., Fugger, L., Göttgens, B., Hacohen, N., Haniffa, M., Hemberg, M., Kim, S., Klenerman, P., Kriegstein, A., Lein, E., Linnarsson, S., Lundberg, E., Lundeberg, J., Majumder, P., Marioni, J. C., Merad, M., Mhlanga, M., Nawijn, M., Netea, M., Nolan, G., Pe'er, D., Phillipakis, A., Ponting, C. P., Quake, S., Reik, W., Rozenblatt-Rosen, O., Sanes, J., Satija, R., Schumacher, T. N., Shalek, A., Shapiro, E., Sharma, P., Shin, J. W., Stegle, O., Stratton, M., Stubbington, M. J. T., Theis, F. J., Uhlen, M., van Oudenaarden, A., Wagner, A., Watt, F., Weissman, J., Wold, B., Xavier, R., and Yosef, N. (2017) And Human Cell Atlas Meeting Participants. The Human Cell Atlas. *eLife 6*, 6.

(2) Dixit, A., Parnas, O., Li, B., Chen, J., Fulco, C. P., Jerby-Arnon, L., Marjanovic, N. D., Dionne, D., Burks, T., Raychowdhury, R., Adamson, B., Norman, T. M., Lander, E. S., Weissman, J. S., Friedman, N., and Regev, A. (2016) Perturb-Seq: Dissecting Molecular Circuits with Scalable Single-Cell RNA Profiling of Pooled Genetic Screens. *Cell 167*, 1853−1866.

(3) Adamson, B., Norman, T. M., Jost, M., Cho, M. Y., Nuñez, J. K., Chen, Y., Villalta, J. E., Gilbert, L. A., Horlbeck, M. A., Hein, M. Y., Pak, R. A., Gray, A. N., Gross, C. A., Dixit, A., Parnas, O., Regev, A., and Weissman, J. S. (2016) A Multiplexed Single-Cell CRISPR Screening Platform Enables Systematic Dissection of the Unfolded Protein Response. *Cell 167*, 1867−1882.

(4) Gerlai, R. (2016) Gene Targeting Using Homologous Recombination in Embryonic Stem Cells: The Future for Behavior Genetics? *Front. Genet. 7*, 43.

(5) Mali, P., Aach, J., Stranges, P. B., Esvelt, K. M., Moosburner, M., Kosuri, S., Yang, L., and Church, G. M. (2013) CAS9 transcriptional activators for target specificity screening and paired nickases for cooperative genome engineering. *Nat. Biotechnol. 31*, 833−838.

(6) Chavez, A., Scheiman, J., Vora, S., Pruitt, B. W., Tuttle, M., Priyer, E., Lin, S., Kiani, S., Guzman, C. D., Wiegand, D. J., Ter-Ovanesyan, D., Braff, J. L., Davidsohn, N., Housden, B. E., Perrimon, N., Weiss, R., Aach, J., Collins, J. J., and Church, G. M. (2015) Highly efficient Cas9-mediated transcriptional programming. *Nat. Methods 12*, 326−328.

(7) Konermann, S., Brigham, M. D., Trevino, A. E., Joung, J., Abudayyeh, O. O., Barcena, C., Hsu, P. D., Habib, N., Gootenberg, J. S., Nishimasu, H., Nureki, O., and Zhang, F. (2015) Genome-scale transcriptional activation by an engineered CRISPR-Cas9 complex. *Nature 517*, 583−588.

(8) Tanenbaum, M. E., Gilbert, L. A., Qi, L. S., Weissman, J. S., and Vale, R. D. (2014) A protein-tagging system for signal amplification in gene expression and fluorescence imaging. *Cell 159*, 635−646.

(9) Horlbeck, M. A., Gilbert, L. A., Villalta, J. E., Adamson, B., Pak, R. A., Chen, Y., Fields, A. P., Park, C. Y., Corn, J. E., Kampmann, M., and Weissman, J. S. (2016) Compact and highly active next-generation libraries for CRISPR-mediated gene repression and activation. *eLife 5*, 5.

(10) Sanson, K. R., Hanna, R. E., Hegde, M., Donovan, K. F., Strand, C., Sullender, M. E., Vaimberg, E. W., Goodale, A., Root, D. E., Piccioni, F., and Doench, J. G. (2018) Optimized libraries for CRISPR-Cas9 genetic screens with multiple modalities. *Nat. Commun. 9*, 5416.

(11) Jost, M., Santos, D. A., Saunders, R. A., Horlbeck, M. A., Hawkins, J. S., Scaria, S. M., Norman, T. M., Hussmann, J. A., Liem, C. R., Gross, C. A., and Weissman, J. S. (2020) Titrating gene expression using libraries of systematically attenuated CRISPR guide RNAs. *Nat. Biotechnol. 38*, 355−364.

(12) Michlits, G., Hubmann, M., Wu, S.-H., Vainorius, G., Budusan, E., Zhuk, S., Burkard, T. R., Novatchkova, M., Aichinger, M., Lu, Y., Reece-Hoyes, J., Nitsch, R., Schramek, D., Hoepfner, D., and Elling, U. (2017) CRISPR-UMI: single-cell lineage tracing of pooled CRISPR-Cas9 screens. *Nat. Methods 14*, 1191−1197.

(13) Jaitin, D. A., Weiner, A., Yofe, I., Lara-Astiaso, D., Keren-Shaul, H., David, E., Salame, T. M., Tanay, A., van Oudenaarden, A., and Amit, I. (2016) Dissecting Immune Circuits by Linking CRISPR-Pooled Screens with Single-Cell RNA-Seq. *Cell 167*, 1883−1896.

(14) Song, Q., Ni, K., Liu, M., Li, Y., Wang, L., Wang, Y., Liu, Y., Yu, Z., Qi, Y., Lu, Z., and Ma, L. (2020) Direct-seq: programmed gRNA scaffold for streamlined scRNA-seq in CRISPR screen. *Genome Biol. 21*, 136.

(15) Replogle, J. M., Norman, T. M., Xu, A., Hussmann, J. A., Chen, J., Cogan, J. Z., Meer, E. J., Terry, J. M., Riordan, D. P., Srinivas, N., Fiddes, I. T., Arthur, J. G., Alvarado, L. J., Pfeiffer, K. A., Mikkelsen, T. S., Weissman, J. S., and Adamson, B. (2020) Combinatorial single-cell CRISPR screens by direct guide RNA capture and targeted sequencing. *Nat. Biotechnol. 38*, 954−961.

(16) Sanjana, N. E., Shalem, O., and Zhang, F. (2014) Improved vectors and genome-wide libraries for CRISPR screening. *Nat. Methods 11*, 783−784.

(17) Nihongaki, Y., Yamamoto, S., Kawano, F., Suzuki, H., and Sato, M. (2015) CRISPR-Cas9-based photoactivatable transcription system. *Chem. Biol. 22*, 169−174.

(18) Kearns, N. A., Genga, R. M. J., Enuameh, M. S., Garber, M., Wolfe, S. A., and Maehr, R. (2014) Cas9 effector-mediated regulation of transcription and differentiation in human pluripotent stem cells. *Development 141*, 219−223.

(19) Guo, J., Ma, D., Huang, R., Ming, J., Ye, M., Kee, K., Xie, Z., and Na, J. (2017) An inducible CRISPR-ON system for controllable gene activation in human pluripotent stem cells. *Protein Cell 8*, 379−393.

(20) Gilbert, L. A., Horlbeck, M. A., Adamson, B., Villalta, J. E., Chen, Y., Whitehead, E. H., Guimaraes, C., Panning, B., Ploegh, H. L., Bassik, M. C., Qi, L. S., Kampmann, M., and Weissman, J. S. (2014) Genome-Scale CRISPR-Mediated Control of Gene Repression and Activation. *Cell 159*, 647−661.

(21) Doench, J. G., Hartenian, E., Graham, D. B., Tothova, Z., Hegde, M., Smith, I., Sullender, M., Ebert, B. L., Xavier, R. J., and Root, D. E. (2014) Rational design of highly active sgRNAs for CRISPR-Cas9-mediated gene inactivation. *Nat. Biotechnol. 32*, 1262−1267.

(22) Labun, K., Montague, T. G., Krause, M., Torres Cleuren, Y. N., Tjeldnes, H., and Valen, E. (2019) CHOPCHOP v3: expanding the CRISPR web toolbox beyond genome editing. *Nucleic Acids Res. 47*, W171−W174.

(23) Stoeckius, M., Zheng, S., Houck-Loomis, B., Hao, S., Yeung, B. Z., Mauck, W. M., 3rd, Smibert, P., and Satija, R. (2018) Cell Hashing with barcoded antibodies enables multiplexing and doublet detection for single cell genomics. *Genome Biol. 19*, 224.

https://dx.doi.org/10.1021/acssynbio.0c00499
ACS Synth. Biol. 2021, 10, 640−645